

Climate shift uncertainty and economic damages

By ROMAIN FILLON, MANUEL LINSSENMEIER AND GERNOT WAGNER*

WORKING DRAFT—DO NOT CITE OR DISTRIBUTE

COMMENTS WELCOME

March 15, 2025

Focusing on global annual averages of climatic variables, as in the standard damage function approach, can bias estimates of the economic impacts of climate change. Here we empirically estimate global and regional dose-response functions of GDP growth rates to daily mean temperature levels and combine them with regional climate projections. We disentangle how much of the missing impacts are due to differences in warming versus heterogeneous damage patterns over space and time. Global damages in 2050 are around 20% higher, when accounting for the shift in the entire distribution of daily mean temperatures at the regional scale. Differences in the shape of daily temperature distributions between climate models transform standard risk rankings based on temperature anomaly, and increase uncertainty across climate models.

JEL: O44, Q54, Q56

Keywords: damage functions, climate risk, uncertainty, climate shift, temporal disaggregation, spatial disaggregation

* Fillon: Université Paris-Saclay, CIRED & PSAE, Paris, France, rfillon@protonmail.com; Linsenmeier: High Meadows Environmental Institute, Princeton University, Princeton, NJ, United States, mlinsenmeier@princeton.edu; Wagner: Columbia Business School, New York, NY, United States, gwagner@columbia.edu

7 Knowing how future climate damages might be distributed in time and space
8 is a key research frontier and policy issue for climate scientists, economists, and
9 decision-makers. The commonly stated rule of thumb: the more disaggregated
10 the data, the higher are the estimated damages [Nordhaus and Yang, 1996, Rudik
11 et al., 2022]. Adaptation may change things, with finer-grained data showing in-
12 creased capacity to adapt [Heutel et al., 2021]. That opens the question around
13 the ‘right’ level of spatial and temporal aggregation for projecting future impacts.
14 Aggregation has advantages, as it comes with statistical robustness, clear iden-
15 tification of causal relationships, and tractability in aggregated models; it also
16 has shortcomings, such as the risk of averaging contradictory effects between re-
17 gions in terms of damage and warming patterns, or hiding uncertainties within
18 or between climate models. Aggregation, thus, might affect risk ranking between
19 models or the magnitude of structural uncertainty across models. Moreover, ag-
20 gregation choices can bias results through unobserved mechanisms.

21 Projections of climate damages in economic models typically rely on reduced-
22 form relationships between climate change and the macroeconomy, which are
23 generally based on *annual* climatic statistics—e.g. mean annual temperatures.
24 Furthermore, models are generally aggregated for that climate variable to be
25 *global*—mean annual global temperatures. Even when disaggregating to regional
26 levels, economists often use global damage functions, instead of using estimates
27 from regional-specific damage patterns. Meanwhile, it seems intuitive that a hot
28 day in a relatively warm country has a different impact than the same day in
29 a cold country; Heutel et al. [2021] show this to be the case for U.S. counties.
30 Moreover, economists often use a linear relationship between global and regional
31 climate that boils down to an annual regional statistic. Annual averages only
32 imperfectly reflect regional-specific shifts in warming patterns. In North-West
33 Europe, for example, hottest summer days are warming twice as fast as mean
34 summer days [García-León et al., 2021, Patterson, 2023].

35 To disentangle these effects, we here follow a two-step approach. First, we

36 switch from annual average temperatures to the complete daily temperature dis-
37 tribution over a year and show how this step affects the heterogeneous distri-
38 bution of warming patterns between regions, compared to a setting where we
39 assume a shape-preserving shift in mean annual temperatures under a changing
40 climate. Second, we interact these regional-specific shifts in warming patterns
41 with regional-specific damage patterns, in comparison with a setting where we
42 assume homogeneous damage patterns at the global scale.

43 Bias-adjusted and gridded climate projections now allow us to compare counter-
44 factual climate to a specific climate scenario at a fine resolution, where ‘climate’ is
45 defined as the underlying distribution, from which a specific regional temperature
46 distribution over a year is drawn [Waidelich et al., 2023]. A large econometric lit-
47 erature has developed in parallel to infer future economic damages from climate
48 change using observed historical impact from past weather [Dell et al., 2014,
49 Hsiang, 2016, Auffhammer, 2018]. This literature often uses disaggregated daily
50 weather data to estimate dose-response functions of an economic variable of inter-
51 est to a summary statistics of the high dimensional climate vector [Hsiang, 2016].
52 But with the notable exception of Rudik et al. [2022], the climate-economic mod-
53 elling literature mostly ignores the shape of region-specific warming and damage
54 patterns and instead focuses on global averages either for warming patterns, or
55 for damage patterns, or for both, regardless of the level of spatial aggregation—
56 from global [Nordhaus, 1994] to regional [Nordhaus and Yang, 1996] and gridded
57 [Cruz and Rossi-Hansberg, 2021, Krusell and Smith Jr, 2022]. This aggregation
58 might have important consequences, both for establishing our best approximation
59 of future damage and in quantifying the uncertainty surrounding this best guess.
60 Uncertainties in climate-economic modelling abound [Rising et al., 2022, Kotz
61 et al., 2023].

62 The quantifiable variance of future projections of climate impacts is affected by
63 scenario uncertainty (differences in SSPs), model uncertainty (differences in ESM
64 responses to the SSPs), internal variability (spatiotemporally, due to the chaotic

65 nature of the climate and due to regional differences that may be hidden by re-
66 gional aggregation), and any choices made in post-processing or bias-correcting
67 ESM output (including how finely to apply projected changes in climate distribu-
68 tions from ESMs), in addition to regression uncertainty from the impact model,
69 and differences between observational data products used to fit the dose-response
70 function and act as a baseline to which future ESM output is compared. Histor-
71 ically, many studies use global annual average climate variables to estimate and
72 project climate damages, thereby ignoring an important source of internal vari-
73 ability stemming from regional differences in climate states and from only extract-
74 ing mean changes from ESM projections. We quantify the sensitivity of economic
75 impact projections to an improved sampling of internal variability (through cap-
76 turing regional differences in impacts) and an improved treatment of ESM output
77 (by capturing changes in the full shape of the temperature distribution instead
78 of annual averages). We take part in uncovering some of the model uncertain-
79 ties between climate models using the whole shape of warming patterns that is
80 usually reduced by the aggregation procedure on a global and annual scale. We
81 provide a framework based on temperature distributions that can be applied to
82 other climate data, and a quantification to show how much the regional-specific
83 shift in the shape of warming patterns interacting with regional-specific damage
84 patterns matter empirically. We then apply this resulting regional climate shift
85 uncertainty to the estimation of future climate damages.

86

87 We first gather climate and economic data, describe region-specific warming
88 patterns for different climate models, and estimate regional damage patterns.
89 We here focus on average surface temperatures, though the framework applies
90 to any number of different statistics that are usually aggregated from daily to
91 annual levels, including e.g. precipitation patterns. In addition, we illustrate our
92 argument for the year 2050, which is sufficiently close so as not to superficially
93 inflate the results, while also being a relevant time horizon for any number of

94 climate policy considerations. Then, we quantify how much the missing shape-
95 related damage of climate change matters for climate policy and provide a simple
96 statistics to operationalize the finding.

97 Our work yields two main conclusions. First, switching from annual global
98 mean temperature to the regional annual distribution of daily mean tempera-
99 tures affects the magnitude of the estimates of economic damages: in 2050, under
100 SSP5-8.5, using regional damage patterns interacted with the shift in the whole
101 shape of the distribution of daily temperatures yields climate damage at the
102 global scale that are around 20% larger than the damage obtained under the as-
103 sumption of homogeneous damage patterns over the world and a shape-preserving
104 shift in annual mean daily temperature. Standard aggregation comes with un-
105 derestimation of future climate damages. Second, we show that the standard risk
106 ranking expressed as the ranking of temperature anomalies between climate mod-
107 els is affected by this shape uncertainty. In SSP5.8-5, the magnitude of scientific
108 uncertainty between climate models is even larger than expected, as standard
109 uncertainty between models is multiplied by shape uncertainty, which further
110 increases dispersion of future possible economic impacts from climate change.

111 I. Climate and economic data

112 A. Warming patterns

113 We compare the distribution of daily mean temperatures in actual climate pro-
114 jections to a counter-factual synthetic projection where the shape of the distri-
115 bution remains the same while the mean annual temperature increases, a stan-
116 dard assumption in the literature. We build different climate landscapes using
117 CMIP6 bias-corrected and downscaled data at a resolution of 60 arc-minutes
118 from five earth system models (ESM) stored in ISIMIP Protocol 3B [Frieler
119 et al., 2023]: GFDL-ESM4, IPSL-CM6A-LR, MPI-ESM1-2-HR, MPI-ESM2-0,
120 UKESM1-0-LL. ISIMIP subset of climate models and de-biasing techniques were
121 designed to assess impacts of climate change and to span the larger ensemble

122 of CMIP models [Warszawski et al., 2014]. Thus, our illustrative study under-
123 estimates inter-model uncertainty among the over 100 CMIP6 models. Data is
124 available for three shared socioeconomic pathways (SSP 1-2.6, 3-7.0, 5-8.5). We
125 construct four different climate landscapes for each SSP. The first is the climate
126 landscape without climate change, the ‘control’ climate: it is the mean distribu-
127 tion of ‘picontrol’ time series experiments run over 2006 to 2100 with pre-industrial
128 CO₂ concentration. The second is the landscape from actual climate projections
129 which consists of bias-corrected, downscaled output from five ESMs forced with
130 future emissions from three different SSPs, the ‘projection’ climate: we use the
131 average of the 10-year distribution around a date to approximately capture the
132 underlying distribution from which the specific weather realization from a spe-
133 cific year is drawn, i.e. 2045-2055 in our example¹. This landscape samples
134 scenario uncertainty, inter-model uncertainty, and regionally specific changes in
135 the shape of daily mean temperature distributions. The third climate landscape
136 is a ‘synthetic-model’ landscape, where we add for each temperature observed in
137 the ‘control’ climate of each of the five ESM the mean of the change in annual
138 temperature in ‘projection’ climate in this specific ESM. This yields a ESM-
139 specific shape-preserving mean-shifted climate. This landscape samples scenario
140 uncertainty, inter-model uncertainty, and regional differences in mean changes,
141 but keeps the shape of daily mean temperature distributions unchanged. The
142 last climate landscape is a ‘synthetic-average’ landscape. The difference with the
143 ‘synthetic-model’ approach is that we sum the mean ‘control’ climate over all
144 ESM and the mean change in annual mean temperature across ESM. This yields
145 a mean shape-preserving, mean-shifted climate, which aggregates heterogeneity
146 between climate models. This landscape samples scenario uncertainty and re-
147 gional differences in mean changes while aggregating across ESMs and keeping

¹On the one hand, adding more years around 2050 would enable us to capture more of the internal variability which characterizes 2050 climate [Schwarzwalder and Lenssen, 2022], for instance more El Niño cycles. On the other hand, it would come with a costly assumption of perfect symmetry around 2050 in climate change dynamics. By capturing less internal variability, we probably under-count the impact of including regional information.

148 the shape of daily mean temperature distributions unchanged.

149 Rather than aggregating this data at the global scale, we construct regional
 150 climate landscapes. Indeed, using a global dataset means that locations in which
 151 a given temperature is relatively cold and places in which the same temperature
 152 is relatively warm in the two locations fall within the same bin of temperature,
 153 which distorts the picture of regional climate shifts, and biases the estimates
 154 used to convert these climate shifts into economic damage. We aggregate at the
 155 level of five major Köppen regions [Beck et al., 2023]: arid, continental, polar,
 156 temperate and tropical. It is reasonable to think that these climate classifications
 157 are both good ensembles in terms of warming patterns but also in terms of damage
 158 patterns to capture differences between relatively homogeneous regions. If the
 159 differences between damage patterns differ for many other reasons (e.g. cultural
 160 and political), we capture some of the regional heterogeneity due to climatic
 161 conditions. A finer disaggregation would reduce the statistical robustness of the
 162 estimates we obtain from our econometric specification below because of limited
 163 sample size and variation. When building these climate landscapes, we keep only
 164 locations for which we have economic data to estimate dose-response functions
 165 below and treat each of these economic region within each climatic Köppen region
 166 as a single unit.

167 *B. Econometric estimates of climate damages*

For the empirical analysis we combine Wenz et al. [2023]’s Database Of Sub-
 national Economic Output (DOSE v2) with Hersbach et al. [2020]’s climate re-
 analysis (ERA5). We process the climate reanalysis by first calculating degree-
 days at the grid-cell level and then aggregating to DOSE regions. We use the
 combined data to estimate global and regional dose-response functions of GDP
 growth to daily mean temperatures. We estimate the model:

$$g_{it} = \alpha_i + P_{it}\beta + \sum_{b=1}^B n_{bit}\gamma_b + \mu_t + \epsilon_{it}$$

168 with the growth rate of GDP per capita PPP in USD in administrative unit i in
 169 year t as g_{it} , with the number of days with daily mean temperature in the bin
 170 indexed b as n_{bit} , and with total annual precipitation P_{it} . Note that here, P_{it}
 171 is indeed only a control, focused on global annual values, rather than regionally
 172 disaggregated daily ones [Kotz et al., 2022]. The model also includes region
 173 fixed effects α_i and year fixed effects μ_t . Errors ϵ_{it} are clustered at the level
 174 of countries to account for spatial and temporal autocorrelation. We estimate
 175 this model for all regions jointly and for each Köppen-Geiger climate zone k
 176 separately. Our main parameters of interest are the coefficients of temperature
 177 bins γ_b (for the global model) and γ_{bk} (for the regional models) which represent
 178 the non-linear association between daily temperature levels and economic growth.
 179 For the regional model, we use a gridded dataset on Köppen climate regions
 180 and assign to every administrative unit the share of each climatic zones it is
 181 included in based on surface area. The 2°C temperature bins are winsorized
 182 at level 99% for econometric estimation to limit the influence of rare events for
 183 which we do not have sufficient observations. Furthermore, we follow Cruz and
 184 Rossi-Hansberg [2021] and smooth the behavior of the point estimates across
 185 temperature bins on the whole temperature distribution in 2050 with degree-
 186 two polynomials, assuming that temperature effect on growth changes remains
 187 constant above and below our upper and lower bins used for the estimation. We
 188 also weigh each point estimate by the inverse of their standard errors to provide
 189 a greater weight to the more accurate estimates.

190 *C. Descriptive statistics*

191 Figure 1 gives summary statistics for the warming and damage patterns of each
 192 region in 2050 for SSP5-8.5. Graphs on the left plot the distribution of mean
 193 daily temperatures for all climate landscapes, taking the average of all five earth
 194 system models. The distributions have different shapes, both in terms of their
 195 dispersion and their mean. The shifts in the average temperature are also of

196 different magnitude, which is consistent with the observation of spatially hetero-
197 geneous global warming. Shifts in shapes are also diverse, and not just because
198 of the initial shape of each distribution as we show on the middle graphs. The
199 middle graphs describe the difference between the ‘synthetic-model’ and the ‘pro-
200 jection’ landscapes for different earth system models: for each 1°C temperature
201 bin, it gives the difference in frequency (in number of days) between two distribu-
202 tions. The first distribution is constructed by adding to each daily temperature
203 for each climate model the mean of the annual anomaly observed in that model,
204 thus obtaining a shape-preserving shift in mean, which is the assumption gener-
205 ally made in the literature. The second distribution is taken from climate model
206 projections of daily mean temperatures. These difference can have opposite signs
207 and various magnitude depending on the model considered. The graphs on the
208 right present the minimum, central and maximum estimates of the two global
209 and regional dose-response functions of GDP growth rate to an additional day in
210 a given bin in comparison with a day in the [20 : 22°C] bin, estimated for each
211 region. Our regional dose-response functions reveals different damage patterns
212 than the global dose-response function. For instance, while the positive effect
213 of colder temperatures on GDP growth in the global functions stills holds with
214 regional estimates in the continental areas, the sign of this effect is reversed for
215 polar and temperate areas. For warmer days, in relatively warmer areas, the
216 effect of higher temperatures goes in both directions, i.e. positive effect for arid
217 areas, negative effects for tropical areas, while it is flat in our global estimate
218 that conflates both climatic zones. Disentangling global and regional damage
219 patterns matter for climate policy because it provides a more accurate picture of
220 the spatial and temporal heterogeneity in future climate damage.

221 More details on the climate shift are given in the heatmap in Figure 3. We
222 plot the number of days under actual projections that are both outside synthetic
223 climate and above the median of its distribution. It is negative (positive) when
224 there are less (more) days in projections that are above the median of synthetic

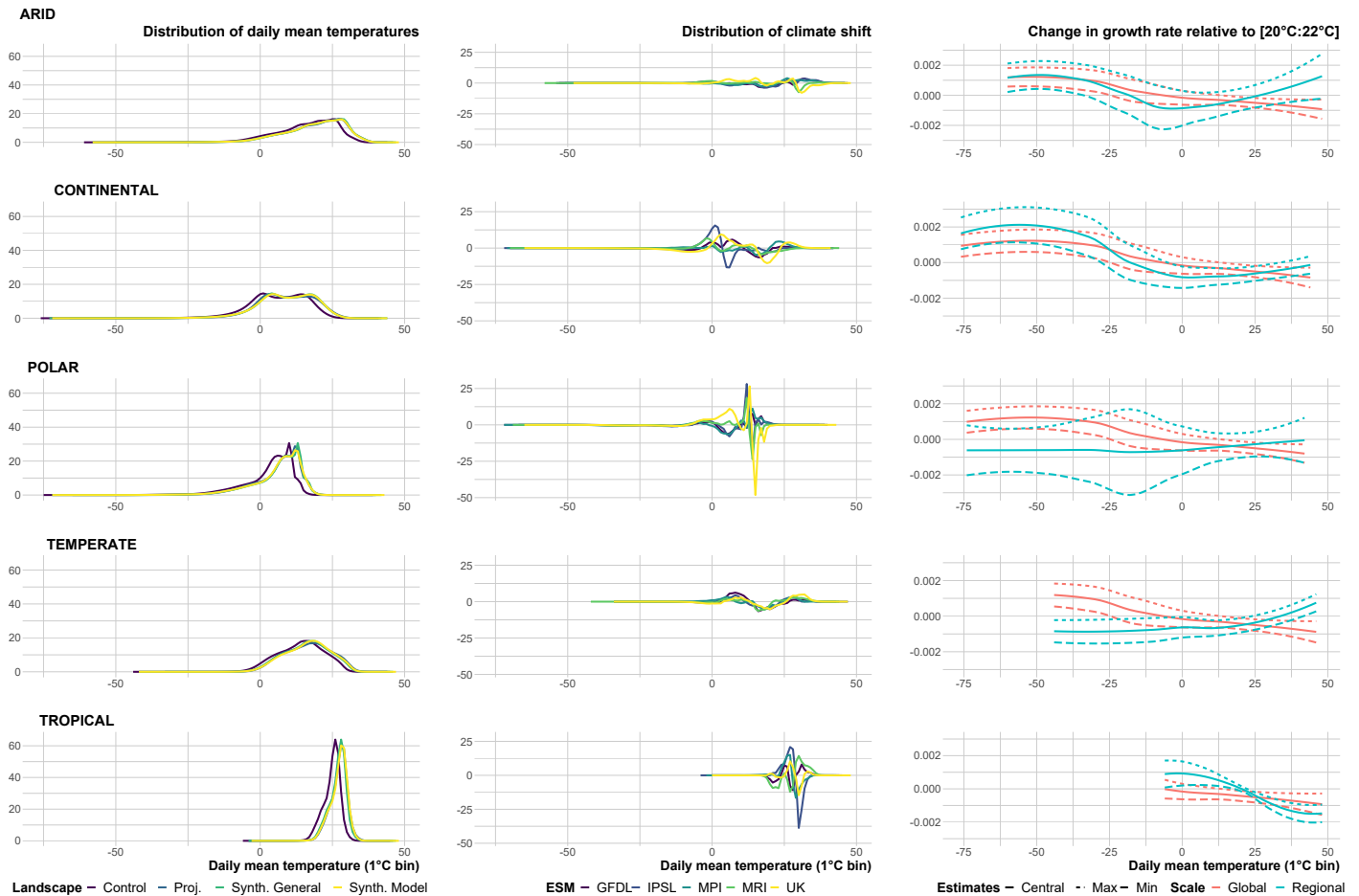


Figure 1. : **Left** Distribution of daily mean temperatures for four climate landscapes. **Middle** Distribution of climate shift, i.e. difference in distribution of daily mean temperatures under projection vs. a synthetic-model climate. **Right** Change in growth rate from one day in this bin relative to one additional day in [20°C : 22°C]. Data are for all DOSE regions, SSP5-8.5, 2050.

225 climate. There is no clear sign for this climate shift: climate projections are not
 226 unequivocally more right-skewed than the synthetic approach. The sign of the
 227 shift is reversed depending on the climate model used.

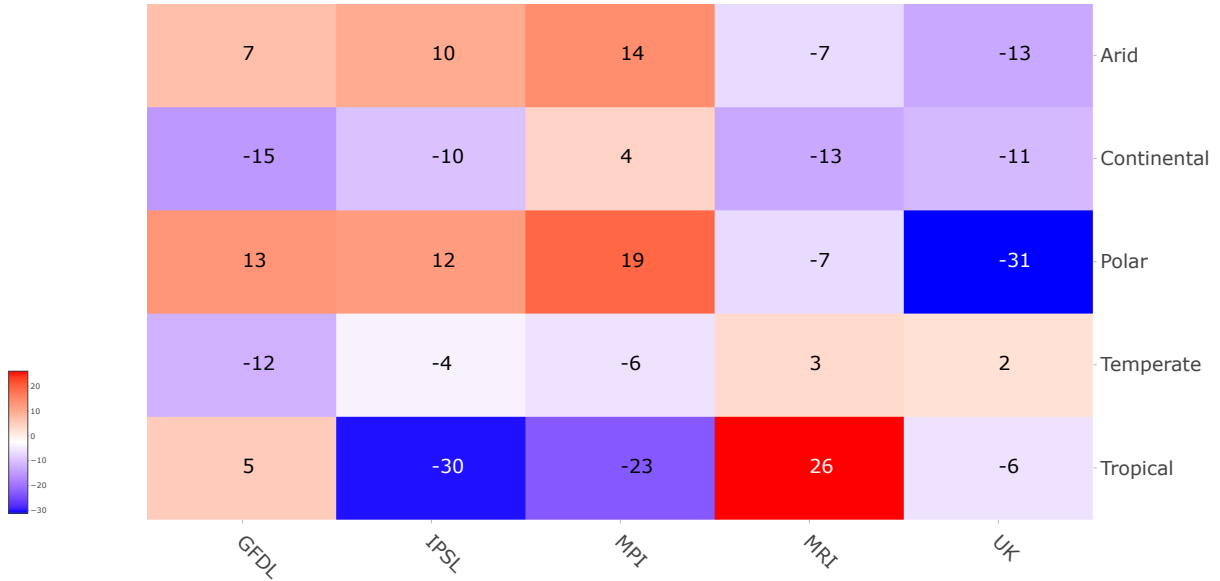


Figure 2. : Days in SSP5-8.5 2050 actual projections for all climate models and DOSE regions that are (1) outside the distribution of synthetic climate and (2) above the median of daily mean temperature distribution in synthetic climate.

228

II. Quantification

229

A. Missing shape-related growth effect of climate change

230

231

232

233

234

235

236

237

238

239

We express the GDP growth effect of daily temperatures in climate projections as a share of this effect in synthetic climate, i.e. in a setting where we assume that the shape of the distribution of daily temperatures remains the same when the mean increases. Indeed, we want to measure how much the change in the shape of the distribution of daily mean temperatures matter for the estimation of economic damages. To have a measure that approaches standard climate damages, growth effects in warming climates are expressed with respect to growth effects in control climate. Growth effect at each 1°C bin b is γ_b (γ_{bk}) if we use global (regional) dose-response functions, where k stands for a Köppen-Geiger climate zone. The global growth effect Ω for a given SSP and year in our climate landscape C for

240 a given dose-response function in subadministrative region DOSE d in Köppen-
 241 Geiger climate zone k is:

$$\Omega_{ymd}^{glob,C} = \frac{(\sum_b \gamma_b t_{bymd}^C - \sum_b \gamma_b t_{bymd}^{control})}{\sum_b \gamma_b t_{bymd}^{control}}, \quad \Omega_{ymdk}^{reg,C} = \frac{(\sum_b \gamma_{bk} t_{bymdk}^C - \sum_b \gamma_{bk} t_{bymdk}^{control})}{\sum_b \gamma_{bk} t_{bymdk}^{control}}$$

242 Then, we apply a double difference procedure to find the change in growth
 243 effect between synthetic climate and projections. For damage function γ , and
 244 synthetic climate: $DD_{ymdk}^\omega = 100 * (\Omega_{ymdk}^{\omega,projection} - \Omega_{ymdk}^{\omega,synthetic}) / \Omega_{ymdk}^{\omega,synthetic}$, with
 245 $\omega \in \{global, regional\}$. This estimate expresses the share the missing shift in
 246 shape represents in the standard estimates of damages assumed from shape-
 247 preserving synthetic shift in mean. We summarize the values of this estimate
 248 for various specifications in Figure 3 below which disentangles various layers of
 249 uncertainty. On the top left graph, we plot the dispersion in our DD estimate
 250 for each Köppen climatic region and each SSP, for each ESM (in blue) and the
 251 average over ESM (in red). This graph captures how for each region the differ-
 252 ences between SSP and between climate models drives the impact omitting the
 253 whole shape of warming pattern has on the assessment of damages. There is an
 254 important climate model uncertainty. Outside continental areas, depending on
 255 the climate model used, the sign of the difference between the standard assump-
 256 tion and the full shape of the distribution is either positive or negative. Part
 257 of this structural uncertainty between climate models is already captured when
 258 comparing climate models at the aggregate annual scale. Thus, on the bottom
 259 left graph, we plot the dispersion between two methods to build our synthetic
 260 climate: either using the model-specific control climate and mean aggregate tem-
 261 perature increase to build the new synthetic benchmark, or using the average over
 262 different ESM. On the top right graph, we plot the difference in our estimates
 263 depending on the dose-response function of GDP growth to daily temperatures
 264 that is used: either the global dose-response function which combines potentially
 265 contradictory effects of changes in temperature distribution over space, or the

266 regional estimates which might capture part of the spatial heterogeneity in dam-
267 age patterns. On the bottom right graph, we plot our coefficient for the central,
268 minimum and maximum estimates of the regional dose-response function to mea-
269 sure how much parametric uncertainty for a given damage function specification
270 matters in comparison with structural uncertainty about the damage function,
271 i.e. either global or regional. The main source of uncertainty that is hidden un-
272 der the assumption of a shape-preserving mean-shifted synthetic climate stems
273 from structural uncertainty across climate models, i.e. heterogeneity in projected
274 regional warming patterns, and structural uncertainty about the shape of damage
275 patterns, i.e. global versus regional damage estimations.

276 *B. Simple statistics for policy-makers*

277 While we build regional climate landscapes that use the granularity given in
278 climate datasets rather than too aggregated information to discuss climate pol-
279 icy, we seek for global indicators that can easily be applied to aggregate economic
280 models. We compute for each DOSE region within each larger Köppen-Geiger
281 zone the share of missing growth due to disaggregated warming and damage pat-
282 terns, either using 2020 GDP [Kummu et al., 2018], or using SSP scenario to
283 compute 2050 GDP of each DOSE region [Wang and Sun, 2022]. We aggregate
284 the DOSE-level growth effect to the global scale based on the share of each zone
285 in global GDP. We use the synthetic-model approach to build a synthetic climate,
286 assuming that aggregate uncertainty between climate model is already taken into
287 account in the literature studying aggregate annual mean temperatures. Indeed,
288 our study focuses on one channel of uncertainty: the interactions between intra-
289 annual warming patterns and damage patterns at the regional scale. On left graph
290 in Figure 4, we plot our estimate of the share of missing growth effects with two
291 approaches: either 2020 GDP or GDP taken from SSP. The underestimation is
292 around 20% lower using SSP projections. On the graph in the middle, we plot
293 our global DD for various ESM and the mean across ESM under regional dam-

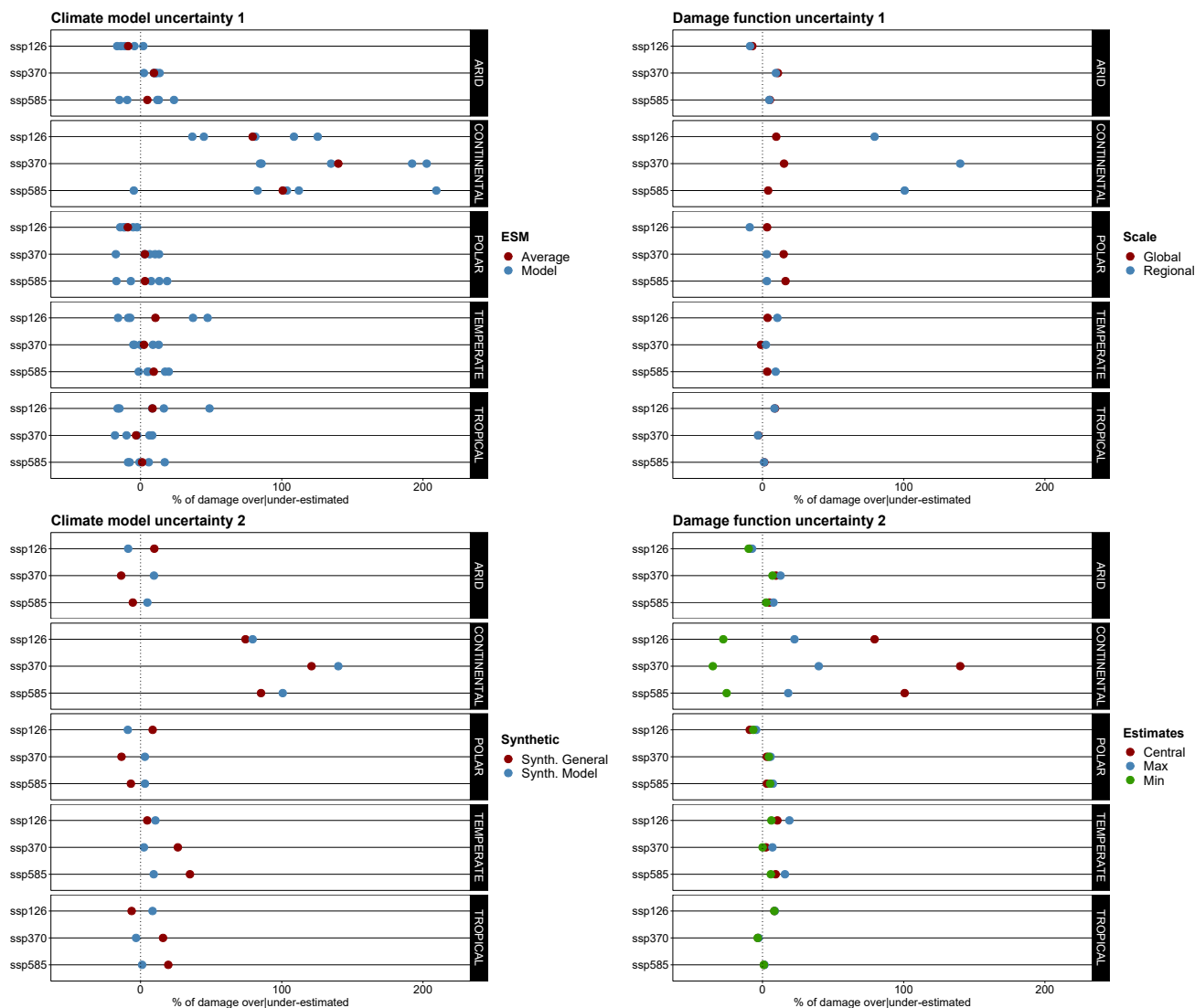


Figure 3. : DD for different specifications, year 2050, all SSP and regions. **Left Top** For each ESM vs. average, using synthetic-model and regional damage **Left Bottom** For synthetic-model vs. synthetic-average, using regional damage, averaging over ESM **Right Top** For global vs. regional damage, using synthetic-model, averaging over ESM **Right Bottom** For central, min. and max. estimates of regional damage, using synthetic-model, averaging over ESM.

294 ages. The dispersion between climate models is larger than the dispersion across
 295 economic scenarii. On the right graph, we plot global DD for two specifications of
 296 the dose-response function: either global or regional. Structural uncertainty on
 297 the damage function matters as the underestimation is around seven times larger
 under regional estimates than under global estimates across the three SSP.

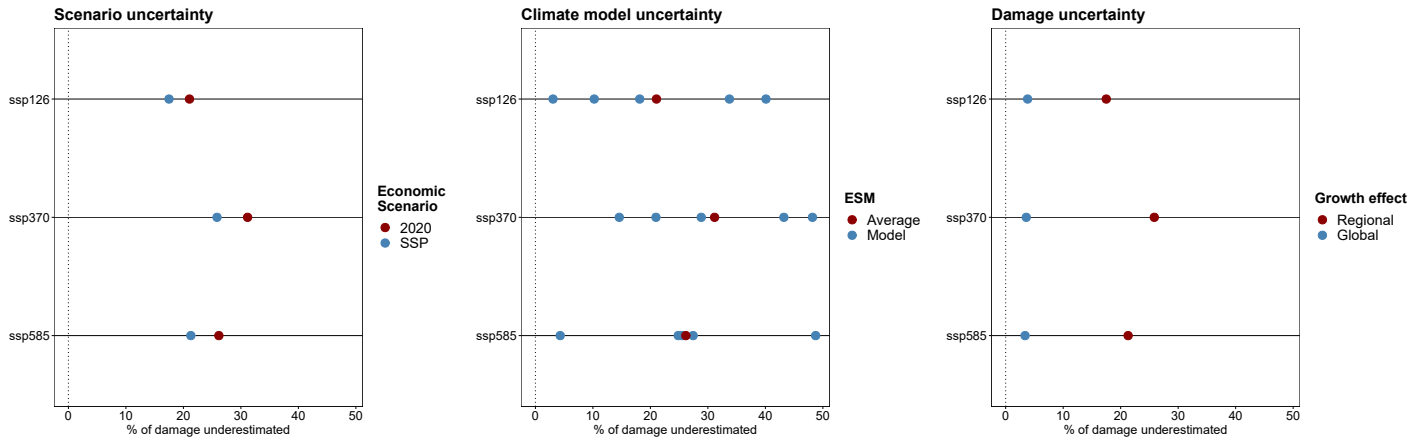


Figure 4. : **Left** Global DD under synthetic-model approach for two aggregation methods, either with 2020 fixed weights or with SSP scenario, for regional damages, average over climate models **Middle** Global DD for each climate model and their average with SSP aggregation method, regional damages **Right** Global DD for each dose-response function and average climate model with SSP aggregation method, regional damages.

298

299 The assumption made in the literature of a shape-preserving shift in mean annual
 300 global temperature interacted with global damage patterns thus yields biased
 301 estimates of future economic damages of climate change. For all climate models
 302 and across various specifications of damage patterns and economic scenarios, this
 303 bias is an underestimation of future damages: accounting for the shift in regional
 304 shape would increase the actual damage by 21.3% under SSP5-8.5 in 2050. The
 305 shift in shape matters also for less carbon-intensive pathways: the underestima-
 306 tion is of 17.5% (25.8%) under SSP1-2.6 (SSP3-7.0). Both uncertainty between
 307 climate models on the shape of regional warming patterns and uncertainty on the

308 damage patterns matter. Their interaction is likely to significantly alter the tem-
 309 poral and spatial distribution of the economic damage caused by climate change.
 310 This modified picture changes mitigation and adaptation policies.

311

312 Part of the dispersion between models highlighted above, which is linked to the
 313 complete shape of the daily temperature distribution, is generally hidden when
 314 we focus on annual average temperatures. This, in turn, is likely to change risk
 315 ranking between models. It can also change the magnitude of uncertainty be-
 316 tween models. In other words, annual global mean temperature is not a sufficient
 317 statistic for climate model uncertainty regarding mean temperatures. In Figure 5,
 318 we plot the ranking of each climate model for two measures: the share of under-
 319 estimated damages highlighted above and the annual mean temperature anomaly
 320 in 2050 for each SSP and at the global scale for all DOSE regions [Wenz et al.,
 2023].

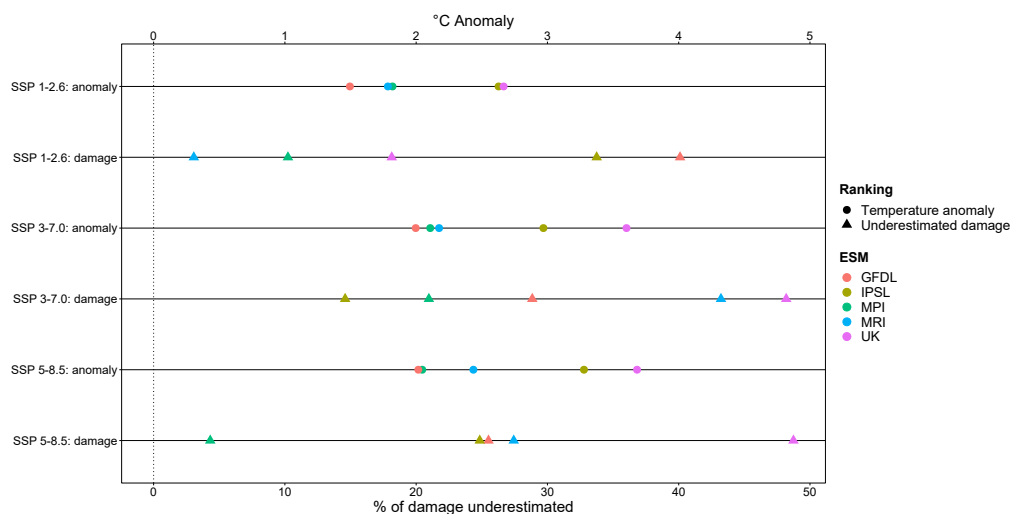


Figure 5. : Risk ranking between climate models for all SSP and all DOSE regions for two key measures: (1) the share of underestimated damage computed with our methodology, (2) the temperature anomaly (in °C).

321

322 The ranking is not always the same: in SSP1-2.6 for instance, GFDL projects
323 the lowest change in temperature anomaly but the distribution of daily tempera-
324 tures in GFDL is the one that deviates furthest from the synthetic distribution,
325 which assumes that the shape of the distribution of daily mean temperatures
326 remains the same. Risk ranking between models in terms of climate impact is
327 likely to be modified in this case. In SSP5.8-5 on the other hand, MPI and UK
328 are the lowest and highest among models for both metrics, which suggest that
329 risk ranking might remain the same, but the magnitude of climate uncertainty
330 between models increases as both uncertainties interact. Indeed, UK has the high-
331 est temperature anomaly over DOSE regions, and the aggregate climate damage
332 computed from this anomaly is multiplied by the largest underestimated share of
333 damage due to climate shift in the shape of the daily temperatures distribution.

334 III. Conclusion

335 If climate-society relationships were linear, then aggregating would not make
336 any difference. But since they are nonlinear, what happens at the regional level
337 matters. Indeed, switching from annual global mean temperature to a regional
338 annual distribution of daily mean temperatures affects the sign and magnitude
339 of economic damages from climate change. This change comes from heterogene-
340 ity in both damage and warming patterns across regions. Disaggregating, thus,
341 reveals how uncertainty between climate models on the whole shape of the distri-
342 bution of future weather realizations cascades down to regional damage estimates.
343 This shape uncertainty affects risk rankings across models and increases the magni-
344 tude of uncertainty between models. Moreover, accounting for daily temperatures
345 rather than annual averages increases the estimation of economic damages, a find-
346 ing consistent with previous studies [Rudik et al., 2022]. In 2050, under SSP5-8.5,
347 using regional damage patterns interacted with the shift in the entire shape of the
348 distribution of daily temperatures, yields climate damages at the global scale that
349 are 20% larger than the damage obtained under the assumption of homogeneous

350 damage patterns over the world and shape-preserving shift in annual mean daily
351 temperature. Climate model uncertainty and damage uncertainty matter more
352 in our setting than economic uncertainty about the share of each region in world
353 GDP in 2050. The shape uncertainty about shifts in daily temperature distribu-
354 tions and regional damage patterns should therefore be taken into consideration
355 for decision-making.

356 To our knowledge, we provide the first comparison between various approaches
357 to spatial and temporal aggregation regarding impacts of changes in mean surface
358 temperatures on economic activity and quantify how much these often-overlooked
359 aggregation procedures matter empirically. We believe that this procedure can
360 be reasonably translated horizontally and vertically. Vertically, this framework
361 can be applied to other economic damages stemming, for instance, from changes
362 in maximum or minimum daily temperatures. Horizontally, the framework can
363 be used to infer results in regions for which we do not have socioeconomic data
364 to estimate damage functions.

365 Our analysis also comes with limitations. In particular, our estimation of re-
366 gional damage functions is based on the idea that differences in the economic dam-
367 age caused by weather—and therefore by climate change—is intimately linked to
368 climatic zones. However, there are many factors that go well beyond geographical
369 determinism that we do not explore here. Furthermore, Earth System Models are
370 imperfect, and some may not be able to capture well the shape (or changes in the
371 shape) of the temperature distribution [Kornhuber et al., 2023]. Finally, while
372 we studied variations of warming patterns in space and time, and variation of
373 damage patterns in space, we have left out the question of variation of damage
374 patterns in time under a ‘swinging climate’ [Mérel et al., 2024]—i.e. adaptation
375 to shifts in climate. How might a given daily temperature yield different damages
376 in any particular region under a different climate, as the region moves away from
377 its normal climatic zone? Lastly, that raises the question of how adaptation might
378 interact with the entire distribution of climatic factors, a question left for further

379 research.

380 REFERENCES

- 381 M. Auffhammer. Quantifying economic damages from climate change. *Journal*
382 *of Economic Perspectives*, 32(4):33–52, 2018.
- 383 H. E. Beck, T. R. McVicar, N. Vergopolan, A. Berg, N. J. Lutsko, A. Dufour,
384 Z. Zeng, X. Jiang, A. I. van Dijk, and D. G. Miralles. High-resolution (1 km)
385 köppen-geiger maps for 1901–2099 based on constrained cmip6 projections.
386 *Scientific data*, 10(1):724, 2023.
- 387 J.-L. Cruz and E. Rossi-Hansberg. The economic geography of global warming.
388 Technical report, National Bureau of Economic Research, 2021.
- 389 M. Dell, B. F. Jones, and B. A. Olken. What do we learn from the weather? the
390 new climate-economy literature. *Journal of Economic literature*, 52(3):740–798,
391 2014.
- 392 K. Frieler, J. Volkholz, S. Lange, J. Schewe, M. Mengel, M. d. R. Rivas López,
393 C. Otto, C. P. Reyer, D. N. Karger, J. T. Malle, et al. Scenario set-up and forc-
394 ing data for impact model evaluation and impact attribution within the third
395 round of the inter-sectoral model intercomparison project (isimip3a). *EGU-*
396 *sphere*, pages 1–83, 2023.
- 397 D. García-León, A. Casanueva, G. Standardi, A. Burgstall, A. D. Flouris, and
398 L. Nybo. Current and projected regional economic impacts of heatwaves in
399 europe. *Nature communications*, 12(1):5807, 2021.
- 400 H. Hersbach, B. Bell, P. Berrisford, S. Hirahara, A. Horányi, J. Muñoz-Sabater,
401 J. Nicolas, C. Peubey, R. Radu, D. Schepers, A. Simmons, C. Soci, S. Ab-
402 dalla, X. Abellan, G. Balsamo, P. Bechtold, G. Biavati, J. Bidlot, M. Bonavita,
403 G. De Chiara, P. Dahlgren, D. Dee, M. Diamantakis, R. Dragani, J. Flem-
404 ming, R. Forbes, M. Fuentes, A. Geer, L. Haimberger, S. Healy, R. J. Hogan,

- 405 E. Hólm, M. Janisková, S. Keeley, P. Laloyaux, P. Lopez, C. Lupu, G. Rad-
406 noti, P. De Rosnay, I. Rozum, F. Vamborg, S. Villaume, and J.-N. Thépaut.
407 The ERA5 global reanalysis. *Quarterly Journal of the Royal Meteorological*
408 *Society*, 146(730):1999–2049, July 2020. ISSN 0035-9009, 1477-870X. doi:
409 10.1002/qj.3803.
- 410 G. Heutel, N. H. Miller, and D. Molitor. Adaptation and the mortality effects
411 of temperature across us climate regions. *Review of Economics and Statistics*,
412 103(4):740–753, 2021.
- 413 S. Hsiang. Climate econometrics. *Annual Review of Resource Economics*, 8:43–75,
414 2016.
- 415 K. Kornhuber, C. Lesk, C. F. Schleussner, J. Jägermeyr, P. Pfliegerer, and R. M.
416 Horton. Risks of synchronized low yields are underestimated in climate and
417 crop model projections. *Nature Communications*, 14(1):3528, 2023.
- 418 M. Kotz, A. Levermann, and L. Wenz. The effect of rainfall changes on economic
419 production. *Nature*, 601(7892):223–227, 2022.
- 420 M. Kotz, A. Levermann, and L. Wenz. The economic commitment of climate
421 change. 2023.
- 422 P. Krusell and A. A. Smith Jr. Climate change around the world. 2022.
- 423 M. Kummu, M. Taka, and J. H. Guillaume. Gridded global datasets for gross
424 domestic product and human development index over 1990–2015. *Scientific*
425 *data*, 5(1):1–15, 2018.
- 426 P. Mérel, E. Paroissien, and M. Gammans. Sufficient statistics for climate change
427 counterfactuals. *Journal of Environmental Economics and Management*, page
428 102940, 2024.
- 429 W. D. Nordhaus. *Managing the global commons: the economics of climate change*,
430 volume 31. MIT press Cambridge, MA, 1994.

- 431 W. D. Nordhaus and Z. Yang. A regional dynamic general-equilibrium model of
432 alternative climate-change strategies. *The American Economic Review*, pages
433 741–765, 1996.
- 434 M. Patterson. North-west europe hottest days are warming twice as fast as mean
435 summer days. *Geophysical Research Letters*, 50(10):e2023GL102757, 2023.
- 436 J. Rising, M. Tedesco, F. Piontek, and D. A. Stainforth. The missing risks of
437 climate change. *Nature*, 610(7933):643–651, 2022.
- 438 I. Rudik, G. Lyn, W. Tan, and A. Ortiz-Bobea. The economic effects of climate
439 change in dynamic spatial equilibrium. 2022.
- 440 K. Schwarzwald and N. Lenssen. The importance of internal climate variability in
441 climate impact projections. *Proceedings of the National Academy of Sciences*,
442 119(42):e2208095119, 2022.
- 443 P. Waidelech, F. Batibeniz, J. A. Rising, J. Kikstra, and S. Seneviratne. Climate
444 damage projections beyond annual temperature. 2023.
- 445 T. Wang and F. Sun. Global gridded gdp data set consistent with the shared
446 socioeconomic pathways. *Scientific Data*, 9(1):221, 2022.
- 447 L. Warszawski, K. Frieler, V. Huber, F. Piontek, O. Serdeczny, and J. Schewe. The
448 inter-sectoral impact model intercomparison project (isi-mip): project frame-
449 work. *Proceedings of the National Academy of Sciences*, 111(9):3228–3232,
450 2014.
- 451 L. Wenz, R. D. Carr, N. Kögel, M. Kotz, and M. Kalkuhl. Dose-global data set
452 of reported sub-national economic output. *Scientific Data*, 10(1):425, 2023.

453 Acknowledgement

454 Romain Fillon thanks the Fulbright Program (France) for funding his research
455 stay at Columbia Business School. The authors thank François Bareille, Adrien

456 Delahais, Célia Escribe, Céline Guivarch, Radley Horton, Adam Sobel and espe-
457 cially Kevin Schwarzwald for fruitful comments on earlier versions of this work.
458 Computations were performed on the Columbia University Research Grid.

459

Appendix A. Building climate landscapes

460

461

462

463

464

465

We scale the frequency of observations by the share of land area in each cell using GPW4 dataset. We compare changes in shapes of daily mean temperature distributions T_{mr} in 5 Koppen regions r and climate model m , i.e. the distribution of all t_{bymr} daily mean temperatures in year y , bin b , region r , model m , in four different climates $C \in \{control, projection, synthetic - model, synthetic - average\}$.

466

- Control climate, without climate change $T_{mr}^{control}$

467

- ISIMIP projections $T_{mr}^{projection}$

468

- Synthetic model with model average

469

$$t_{bymr}^{synthetic-model} = t_{bymr}^{control} + mean_b(t_{bymr}^{projection} - t_{bymr}^{control})$$

470

- Synthetic model with total average

471

$$t_{byr}^{synthetic-average} = mean_m(t_{byr}^{control}) + mean_{bm}(t_{bymr}^{projection} - t_{bymr}^{control})$$

472

Let us define a climate shift indices: $CSI_{bymr} = t_{bymr}^{projections} - t_{bymr}^{synthetic-model}$.

473

474

The Köppen region of use are:

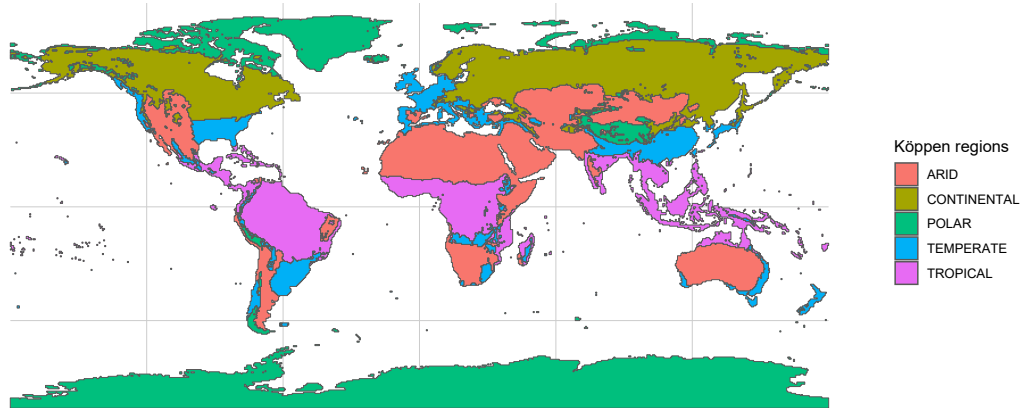


Figure 6. : Köppen climatic zones.

Appendix B. Some graphs

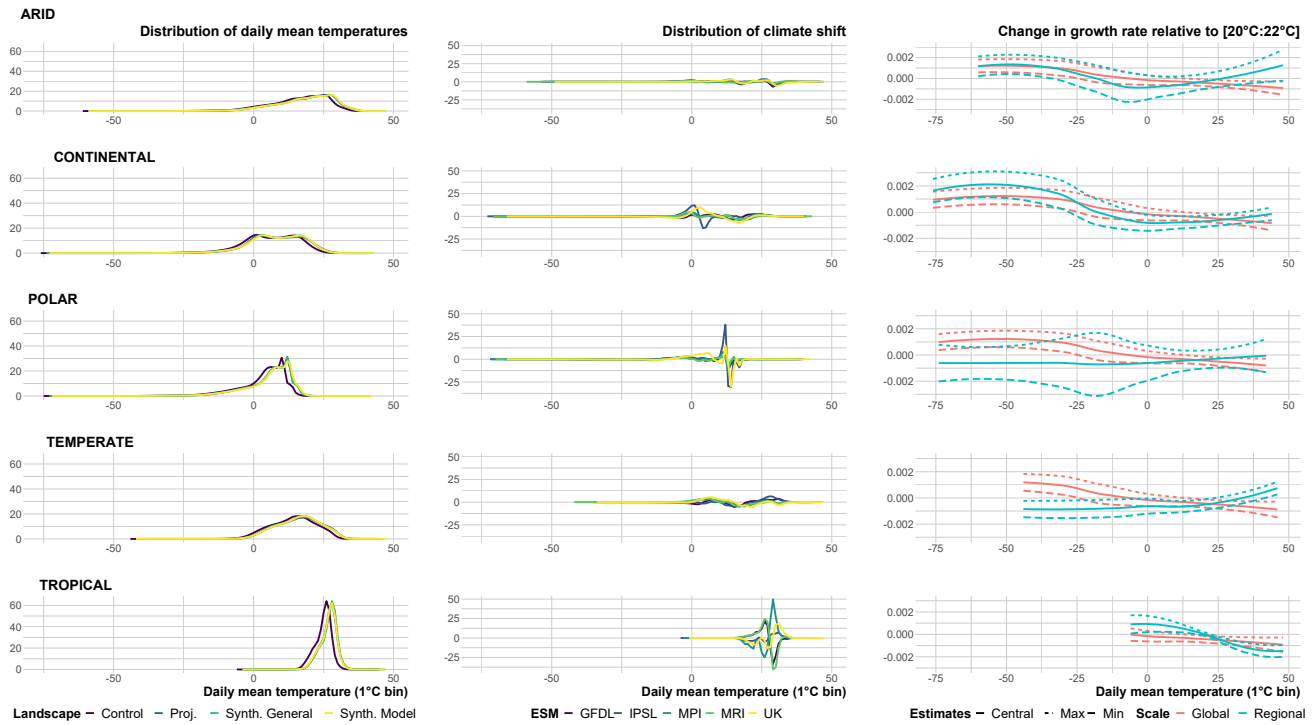


Figure 7. : SSP1-2.6 **Left** Distribution of daily mean temperatures for four different climate landscapes. **Middle** Distribution of climate shift, i.e. difference in distribution of daily mean temperatures under projection vs. a synthetic-model climate. **Right** Change in growth rate from one day in this bin relative to one additional day in [20°C : 22°C].

476

Appendix D. Final statistics

477 We give the values for the share of each climatic region in GDP for different
 478 scenarii used in this paper: either fixed 2020 GDP share, or SSP-dependent GDP
 479 share. From GDP gridded data at 5 arc-min resolution: GDP is upscaled based
 480 on surface area for grid zones that are spread over several Köppen regions.

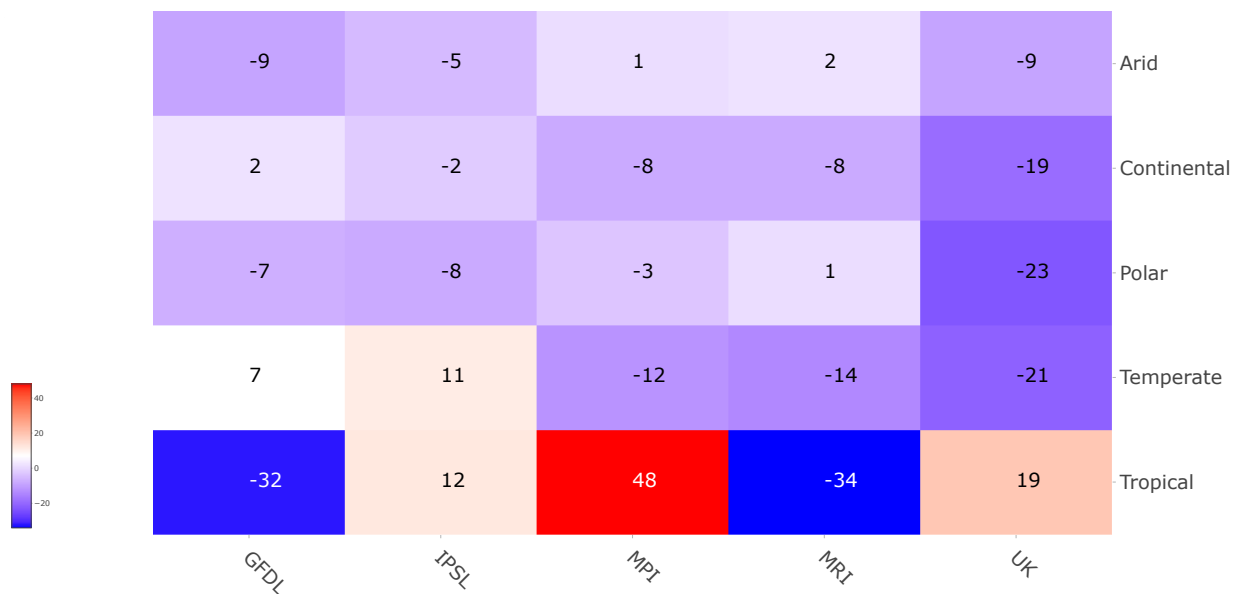


Figure 8. : Heatmaps for SSP1-3.6 year 2050 actual climate projections, for all climate models and regions. Number of days both outside the synthetic-climate distribution and above its median.

Table 1—: Share of each Köppen-Geiger zone k in world's GDP under various assumptions

Region	Arid	Continental	Polar	Temperate	Tropical
2020	0.17	0.206	0.003	0.479	0.142
SSP1	0.176	0.158	0.002	0.444	0.22
SSP3	0.188	0.169	0.002	0.446	0.196
SSP5	0.178	0.16	0.002	0.441	0.219

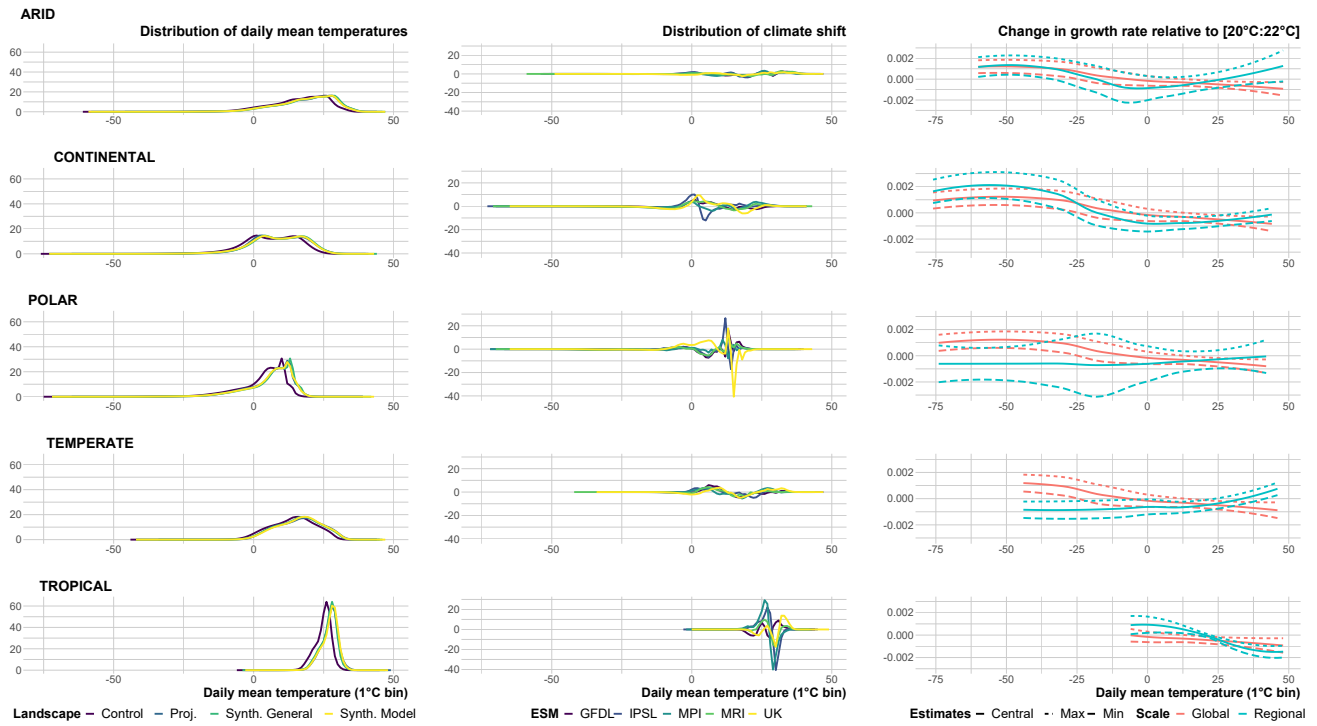


Figure 9. : SSP3-7.0 **Left** Distribution of daily mean temperatures for four different climate landscapes. **Middle** Distribution of climate shift, i.e. difference in distribution of daily mean temperatures under projection vs. a synthetic-model climate. **Right** Change in growth rate from one day in this bin relative to one additional day in [20°C : 22°C].

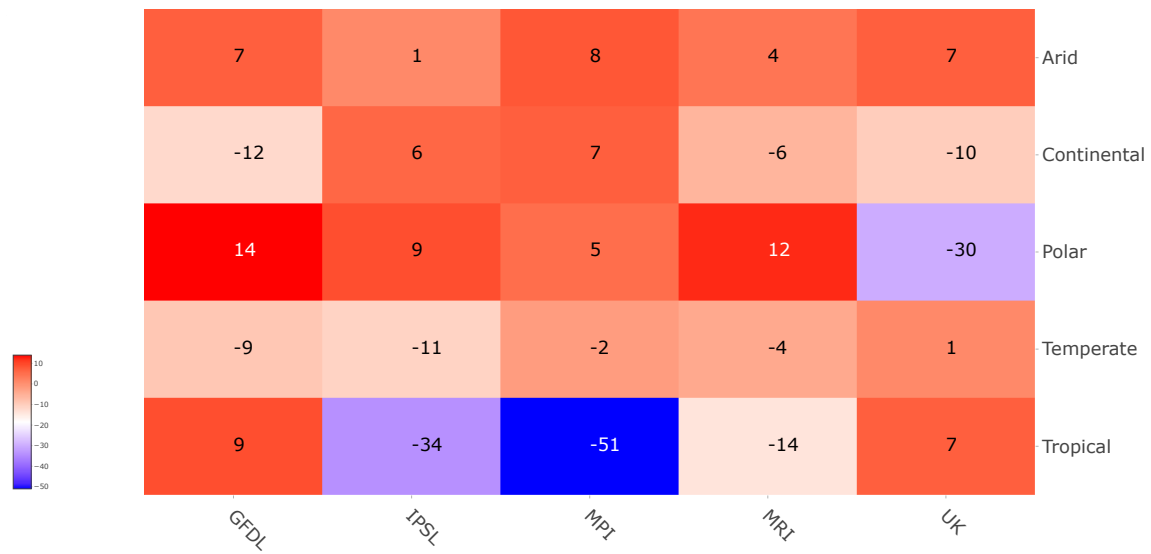


Figure 10. : Heatmaps for SSP3-7.0 year 2050 actual climate projections, for all climate models and regions. Number of days both outside the synthetic-climate distribution and above its median.